Chalcogenide Letters Vol. 17, No. 1, January 2020, p. 19 - 23

SPECTRAL DEPENDENCE OF PHOTOINDUCED FORMATION OF SURFACE RELIEF GRATINGS IN AMORPHOUS CHALCOGENIDES

M. REINFELDE*, J. TETERIS, R. GRANTS
Institute of Solid State Physics, University of Latvia, Latvia

The surface relief grating formation in As_2S_3 and $As_{40}S_{15}Se_{45}$ films under laser wavelengths λ = 491, 532, 561, 594 and 633 nm light influence was examined. The studies of spectral dependence of photoinduced birefringence and its development during the holographic recording in studied chalcogenide films showed that photoinduced birefringence plays an important role in SRG formation process.

(Received September 30, 2019; Accepted January 6, 2020)

Keywords: Amorphous chalcogenide films, Holographic recording, Surface relief gratings

1. Introduction

Phenomenon of direct surface structure formation by holographic recording is caused by photoinduced mass transport under polarized light illumination. The surface relief grating (SRG) direct formation by two coherent laser beam interference recently are studied intensively in various disordered materials such as amorphous inorganic chalcogenides [1-4] and organic azobenzene compounds [5,6]. Efficiency of recording is defined by distribution of electric field vector of resulting interference pattern inside the recording media [1,2]. Formation of SRG on the chalcogenide semiconductor films strongly depends on the polarization state of the recording beams [2, 4, 7-9]. The largest SR modulation can be obtained with $+45^o$: -45^o and RCP: LCP recording beam configurations. Obtained results suggested that the whole illuminated volume of the film takes part in SRG formation process [10-13]. More profound studies showed the SRG formation dependencies on film thickness and grating period. Thus, for layers of As2S3 with thicknesses d≈1.3 μm and 7 μm, optimum grating periods Λopt ≈ 5 ÷ 10 μm and Λopt ≈15 ÷ 20 μm were obtained by recording with λ = 532 nm laser light, respectively [11]. The strong grating period influence on surface relief formation was observed in $As_{40}S_{15}Se_{45}$ films under λ=532 nm laser light illumination although on the layers with limited thicknesses [12]. There the difference in absorption and consequently light penetration depth ρ should be noting for these two compounds. So, ρ calculated following Beer-Lambert law gives ~3 μm and ~0.13 μm for As_2S_3 and $As_{40}S_{15}Se_{45}$ accordingly [14]. Nevertheless, even for such a short penetration depth in $As_{40}S_{15}Se_{45}$ films under λ=532 nm laser light illumination, under certain conditions it is possible to create reliefs with profile high Δh comparable and even exceeding the value of ρ. As one of the factors affecting the manifestation of given effect, we should take in account the interaction between surface tension and surface relief grating formation forces due to light intensity and electric field gradient parallel as well perpendicularly to the film plane. So that should lead to the weakening of surface grating formation driving forces in the direction of larger grating periods from one side and in the direction of light penetration decreasing at growing absorption from the other side[12]. Besides, it should not be excluded the influence on electric field distribution from the side of higher order diffracted beams developing during the recording process inside the films volume when the light penetration depth is sufficiently large.

In this work we present the results of SRG formation studies under influence of different recording wavelength 491<λ<633 covering the range of light penetration depths in the As_2S_3 and $As_{40}S_{15}Se_{45}$ films.

* Corresponding author: mara.reinfelde@cfi.lu.lv

2. Experimental

In these studies the principal attention was devoted to the kinetics of light diffraction during the surface structure formation by holographic recording on non-annealed As_2S_3 and $As_{40}S_{15}Se_{45}$ films. Films were prepared by thermal deposition in vacuum on glass substrate, with thickness controlled by optical interferometer method during the deposition process. All experiments were realized at room temperature.

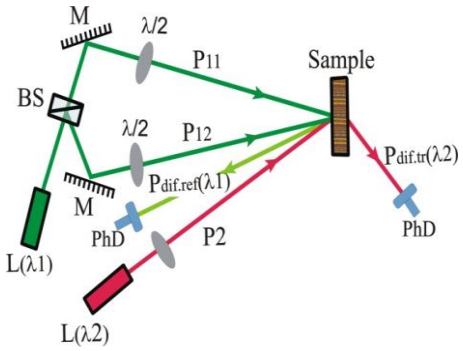

Fig. 1. Recording scheme and conditions: L(λ1) and L(λ2) recording and probing light-wave lasers, BS – beam splitter, M – mirrors, λ/2 – half wave plates, PhD – photo-diodes; P11, P12 – recording light beams, P2-probing light beam, Pdif.ref(λ1) and Pdif.tr(λ2) – diffracted in reflection mode from film surface and diffracted in transmission mode light beams; recording light beam polarization ± 45°; probing light beam polarization s or p.

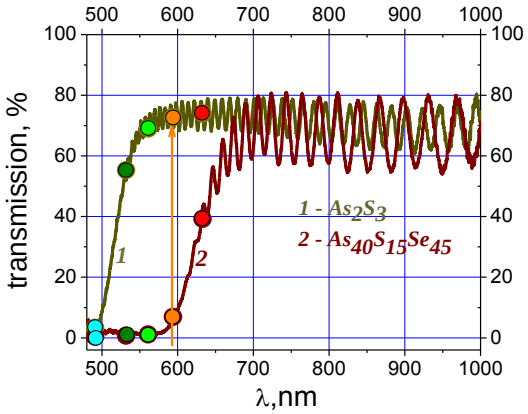

Fig. 2. Transmission spectra of 7 μm thick As_2S_3 and 3,2 μm thick $As_{40}Se_{15}S_{45}$ sample. Circles correspond to wave-length position for lasers used in presented studies. Arrow corresponds to wave-length 594 nm position.

The surface relief grating (SRG) recording was performed with two orthogonally +45°: –45° linearly polarized laser beams of equal intensities I1=I2. SRG recording process was controlled following the kinetics of reflected diffracted light at the recording wave-length (λ1) and using the non-destructive probing wave-length (λ2) beam Figure1. The surface relief grating formation in As2S3 and $As_{40}S_{15}Se_{45}$ films under laser wavelength λ = 491, 532, 561, 594 and 633 nm light influence were examined. The transmission spectra for films used in presented studies are shown in Fig. 2. The appropriate laser wavelengths used in experiments are marked with circles.

The dependences of SRG efficiencies on recording laser wave-length in this article is displayed mainly for grating period Λ≈ 1 μm. The SRG profile was examined by AFM after recording at constant illumination doses. Analysis of recording kinetics was performed for p- and s-polarised red light probing beam diffraction corresponding Bragg's conditions. Following

Kogelnik's formula [15], on the base of values achieved for red light diffraction in transmission mode, the calculations of photo-induced changes of refraction index were realized as

$$\Delta n = arcsin\sqrt{\eta}\frac{\lambda cos\theta}{\pi d},$$

where Δn - changes of refraction index, λ – probing beam wave-length, η – diffraction efficiency, θ – angle of incidence.

3. Results

As we noted earlier the main stage of SRG formation process begins when the film darkening by illumination is nearly finished [10]. On the curves of diffraction that corresponds to small maxima for illumination doses some tenth to even hundreds J/cm^2, see Figures3 and 4. As more detailed analysis shown, this maximum is more or less pronounced in dependence of recording conditions. At very beginning of recording where the recording dose E not exceed 10 J/cm2 (with corresponding recording time some ~seconds), in diffraction curve we note the signs of one maximum more. Taking in account, that these maximums appears at very beginning of recording, we pay the special attention to exclude the influence of phone illumination or interference conditions of thin films.

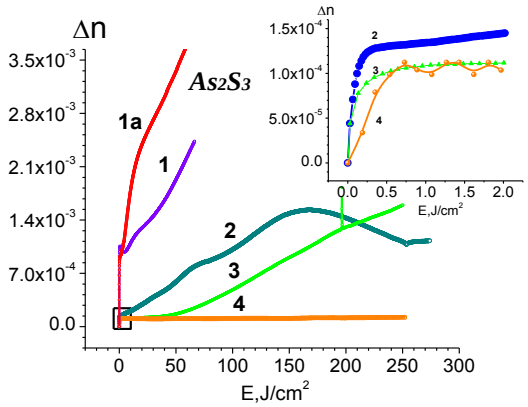

Fig 3. The refraction index Δn dependence on exposure in As_2S_3 films at recording wave-length: 1- λ=491 nm, 2- λ=532nm^2, 3 - λ=561nm, recording light intensity $I_1=I_2\approx0.5$ W/cm^2 4 - λ=594nm $I_1=I_2\approx1.3$ W/cm^2; grating period Λ≈1μm; inset shows the beginning stage of recording up to E≈2.0 J/cm^2; probing beam wave-length λ=653nm polarization-p; 1a – probing beam polarization – s.

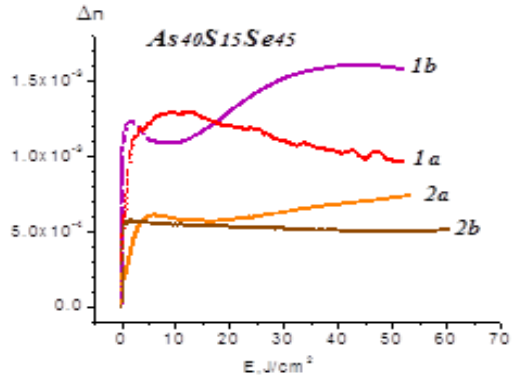

Fig. 4. The refraction index Δn dependence on exposure in $As_{40}S_{15}S_{45}$ films at recording wave-length: 1- λ=635 nm 2- λ=594 nm; light intensity $I_1=I_2\approx0.2$ W/cm^2, grating period Λ≈1μm; curves 1a and 2a shows Δn determinate traditionally; 1b and 2b – calculated through Kogelnik's formula

Calculated photo-induced refraction index changes Δn in dependence on energy dose at the beginning stage of recording where, as we proposed earlier, the mass transportation hasn't started yet is shown in Fig. 3 and Fig. 4. Here are the results which mainly refer to reading with p-polarized probing light beam; reading with s-polarized light beam is presented at curve 1a. The Δn values at the onset peak are comparable for both polarization states. As recording continues, values for s-polarization exceed those for p-polarization; the difference in the linear part remains practically unchanged.

In the Fig. 5 and Fig. 6 it is shown the calculated Δn at exposure E≈1.0 J/cm^2 for As_2S_3 and $As_{40}Se_{15}Se_{45}$ films as well surface relief depth Δh at exposure E≈4.0 kJ/cm^2 in dependence of recording wavelength. As we can see, the curvature of dependencies is similar. For SRG formation as well for Δn in As_2S_3 films at wave-length used in our studies more favorable appear λ = 491 μm. At the wavelength λ =561 nm and 594 we observed only slight symptoms (Δh~ 5μm) of SRG formations. In $As_{40}Se_{15}Se_{45}$ films Δn values calculated at the very beginning stage of recording and fixed at equal intensities surface relief depth grows in direction of higher wavelength.

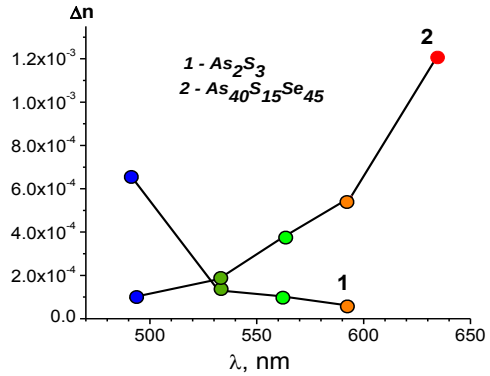

Fig. 5. Dependence of the refraction index changes Δn on recording wave-length in As_2S_3 and $As_{40}Se_{15}Se_{45}$ films at constant exposure E≈1.0 J/cm^2; recording light intensity I_1=I_2≈0.5W/cm^2, grating period Λ=1μm.

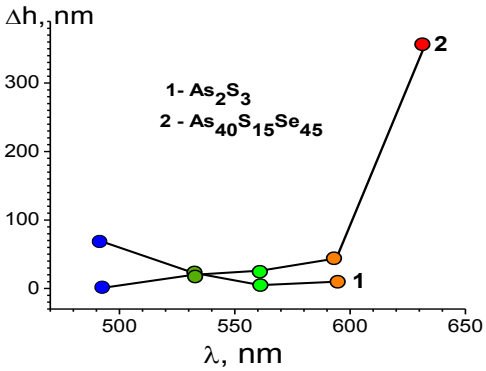

Fig. 6. Dependence of the profile depth Δh on recording wave-length in As_2S_3 and $As_{40}Se_{15}Se_{45}$ films at constant exposure E≈4.0 kJ/cm^2; recording light intensity I_1=I_2≈0.5 W/cm^2; grating period Λ≈1μm. In the As_2S_3 film recording at wave length 594 nm was performed at I_1=I_2≈ 1.4 W/cm^2.

4. Discussion

Looking at the presented results in relation to penetration depth ρ, course of Δh dependencies for $As_{40}Se_{15}Se_{45}$ films goes in acceptable way – at smaller values of ρ, lower of Δh values and vice versa. In As_2S_3 decrease of Δh at longer wavelengths (λ = 561 nm and 591 nm) obviously could be explained with weakening of absorption what does not provide sufficient

softening of recording medium to achieve an effective SRG formation. However at the wavelength $\lambda = 491$ nm where we had to expect Δh to decrease, we observed an increase.

Taking in account results of our studies we can make some speculations about the connection of Δn at the beginning of recording and surface relief formation. Firstly, the observed similarity in curvature of calculated Δn and measured Δh values could show that exactly the changes of Δn in beginning stage of recording indicate on expected possibility for surface relif formation. We propose that at first stage fast reorientation of disordered structural elements [16] in electric field created by recording light waves takes place and are responsible for following surface relief formation. With the softening of material these structural elements (moieties) are transported in the gradient of electric field forming the surface relief. We assume that the changes in Δn observed at the beginning of the recording refer to photoinduced birefringence, but further refers to the change in refractive index in volume due to absorption.

5. Conclusions

The direct surface relief gratings formation in thin films of chalcogenide semiconductor As_2S_3 and $As_{40}Se_{15}Se_{45}$ films at laser wave-lengths $\lambda = 491$, 532, 594 and 633 nm was studied. The best SRG formation efficiency for As_2S_3 and $As_{40}Se_{15}Se_{45}$ films was observed at recording by $\lambda =$ 491μn and 633 μm light, respectively. The connection of photo induced birefringence with surface relief formation is shown.

References

[1] A. Saliminia, T. V. Galstian, A .Villeneuve, Phys.Rev. Lett. **85**, 4112 (2000).
[2] K. E. Asatryan, T. Galstian, R. Vallee, Phys. Rev. Lett. **94**, 087401 (2005).
[3] S. Kokenyesi, I. Ivan, V. Takats, J. Palinkas, S. Biri, I. A. Szabo, Journ. Non-Cryst. Solids **353**, 147 (2007).
[4] U. Gertners, J. Teteris, Opt. Mat. **32**, 807 (2010).
[5] P. Rochon, E. Batalla, A. Natansohn, Appl. Phys. Lett. **66**, 136 (1995).
[6] B. Bellini, J. Ackermann, H. Klein, Ch. Graves, Ph. Dumas, V. Safarov, J. Phys. Cond. Matter **18**, 1817 (2006).
[7] V. M. Kryshenik, M. L. Trunov, V. . Ivanitsky, J. Optoelectron. Adv. M. **9**, 1949 (2007).
[8] M. Reinfelde, J. Teteris, J. Optoelectron. Adv. M. **13**, 1531 (2011).
[9] J. Teteris, U. Gertners, M..Reinfelde, J. Phys. Status Solidi C **8**, 2780 **(**2011).
[10] M. Reinfelde, R. Grants, J. Teteris J Phys. Status Solidi C **9(**12), 2586 (2012).
[11] M. Reinfelde, J Teteris, E Potanina Can. J. Phys. **92**, 659 (2014).
[12] M. Reinfelde, J. Teteris Journ Non-cryst.Solids **377**, 162 (2013).
[13] J. Teteris, U. Gertners, IOP Conf. Series: Mat. Sc. Engineering **38**, 012012 (2012).
[14] M. Reinfelde, L. Loghina, Z. Ivanova, J. Teteris, U.Gertners, S. Slang, M. Vlcek, J. Optoelectron. Adv. M. **18**, 1 (2016).
[15] H. Kogelnik, Bell Syst. Tech. Journ. **48**, 2909 (1969).
[16] Keiji Tanakaa, Koichi Shimakawa, Journ. Non-Cryst. Sol. **481**, 579 (2018).